# GC-MS Analysis, Bioactivity-based Molecular Networking and Antiparasitic Potential of the Antarctic Alga *Desmarestia antarctica*



Authors

**Gustavo Souza dos Santos[1], Karen Cristina Rangel[2], Thaiz Rodrigues Teixeira[1], Lorena Rigo Gaspar[2], Péricles Gama Abreu-Filho[3], Luíz Miguel Pereira[3], Ana Patrícia Yatsuda[3], Marília Elias Gallon[1], Leonardo Gobbo-Neto[1], Leandro da Costa Clementino[5], Márcia Aparecida Silva Graminha[4], Laís Garcia Jordão[6], Adrian Martin Pohlit[6], Pio Colepicolo-Neto[7]*, Hosana Maria Debonsi[1]***

Affiliations

1 Department of Biomolecular Sciences, School of Pharmaceutical Sciences of Ribeirão Preto, University of São Paulo, Ribeirão Preto, SP, Brazil
2 Department of Pharmaceutical Sciences, School of Pharmaceutical Sciences of Ribeirão Preto, University of São Paulo, Ribeirão Preto, SP, Brazil
3 Department of Clinical Analysis, Toxicology and Food Science, School of Pharmaceutical Sciences of Ribeirão Preto, University of São Paulo, Ribeirão Preto, SP, Brazil
4 Department of Clinical Analysis, School of Pharmaceutical Sciences of São Paulo State University Júlio de Mesquita Filho, Araraquara, SP, Brazil
5 Institute of Chemistry, State University Júlio de Mesquita Filho, Araraquara, SP, Brazil
6 Technology and Innovation Department, National Institute of Amazon Research, Manaus, AM, Brazil
7 Chemistry Institute, University of São Paulo, São Paulo, SP, Brazil

Key words

desmarestiaceae, desmarestia antarctica, leishmania amazonensis, neospora caninum, plasmodium falciparum, antiparasitic, molecular targets and activities, marine macroalgae

**received** 06.05.2020
**revised** 20.06.2020
**accepted** 13.07.2020

Bibliography

**DOI** https://doi.org/10.1055/a-1219-2207
Planta Med Int Open 2020; 7: e122–e132

ISSN 2509-9264

Correspondence

Prof. Dr. Hosana Maria Debonsi
Departamento de Ciências Biomoleculares, Faculdade de Ciências Farmacêutica de Ribeirão Preto, Universidade de São Paulo
Avenida do Café s/n
Ribeirão Preto
São Paulo
14040-903
Brasil
Tel.: + 55 16 3315 4713, Fax + 55 16 3315 4243
hosana@fcfrp.usp.br

Supporting Information for this article is available online at http://www.thieme-connect.de/products.

## ABSTRACT

Leishmaniasis, malaria, and neosporosis are parasitic diseases that affect humans and animals, causing public health problems and billions in economic losses. Despite the advances in the development of new drugs, the severe side effects of available leishmaniasis treatments, the *Plasmodium* spp. resistance to antimalarial drugs, and the lack of a specific treatment against neosporosis lead us to the search for new anti-protozoan molecules from underexplored sources such as the Antarctic marine environment. Herein, we describe for the first time the chemical profile of *Desmarestia antarctica* crude extract and fractions using GC-MS and LC-MS/MS (molecular networking) approaches, and evaluate their antiparasitic activity against *Leishmania amazonensis*, *Neospora caninum*, and multi-drug-resistant *Plasmodium falciparum*. Furthermore, the cytotoxicity in 3T3 BALB/c fibroblasts and Vero cells was evaluated. *D. antarctica* fraction E ( $IC_{50}$ of 53.8 ± 4.4 µg $mL^{-1}$ and selectivity index of 3.3) exhibited anti-promastigote activity and was fourfold more selective to *L. amazonensis* rather than to the host cells. *D. antarctica* fraction D ($IC_{50}$ of 1.6 ± 1.3 µg $mL^{-1}$ and selectivity index of 27.8), *D. antarctica* fraction F ($IC_{50}$ of 3.1 ± 2.1 µg $mL^{-1}$ and selectivity index of 23.1), and *D. ant-*

* These authors contributed equally to this work.

*arctica* fraction H ($IC_{50}$ of 3.1 ± 2.0 µg $mL^{-1}$ and selectivity index of 12.9) presented the highest antiparasitic effects against *N. caninum* with no cytotoxic effects. Also, *D. antarctica* fraction D presented a significant antiplasmodial inhibitory effect ($IC_{50}$ of 19.1 ± 3.9 µg $mL^{-1}$ and selectivity index of 6.0). GC-MS analysis indicated palmitic acid, myristic acid, fucosterol, phthalic acid, di(2-methylbutyl) ester, loliolide, and neophytadiene as the main components in the active fractions. In addition, this is the first report of a biological screening of macroalgae secondary metabolites against *N. caninum* parasites.

**ABBREVIATIONS**

| | |
|---|---|
| VLC: | vacuum liquid chromatography |
| NPs: | natural products |
| DA-FD: | *Desmarestia antarctica* fraction D |
| DA-FE: | *Desmarestia antarctica* fraction E |
| DA-FF: | *Desmarestia antarctica* fraction F |
| DA-FG: | *Desmarestia antarctica* fraction G |
| DA-FH: | *Desmarestia antarctica* fraction H |
| DA-FI: | *Desmarestia antarctica* fraction I |
| FA: | fatty acid |
| SI: | selectivity index |

## Introduction

Humans and animals are host to a myriad of protozoan parasites that cause severe public health problems and affect millions of people throughout the world, costing billions of dollars for developing countries each year [1].

Leishmaniasis is found in about 89 countries and accounts for 1.5 to 2 million new cases annually and causes approximately 70 000 deaths per year. The treatment consists of chemotherapeutic agents such as the pentavalent antimonials amphotericin B, paromomycin, and miltefosine. However, the effectiveness of these drugs is holdback by its severe side effects [2].

The phylum Apicomplexa includes several important human and animal disease-causing parasites, including the agents of human malaria *Plasmodium* spp. and the animal agent of neosporosis, *Neospora caninum* [3]. *N. caninum* infects mammalian species, including cattle, sheep, goats, horses, and dogs, and despite the effort of many research groups and industry, neosporosis lacks an effective chemotherapy, leading to relevant economic losses mainly in developing and underdeveloped countries since the parasite is related to an abortive syndrome in cattle [5].

Human malaria is caused by four different species of *Plasmodium* spp., but the severe form is caused by *Plasmodium falciparum* [3]. There were an estimated 219 million cases and 43 500 deaths related to the disease in 2017 [6]. Malaria chemotherapy is effective and nontoxic but protozoa resistance to antimalarial drugs became a debilitating point towards its control and elimination [7]. The new drug artefenomel, a novel synthetic trioxolane antimalarial drug, is currently in phase 2 clinical tests [8], but with regard to the rapidly acquired *Plasmodium* spp. resistance to antimalarial drugs, the search for bioactive compounds against this parasite needs to be continued.

NPs have been used by humans through the ages [9] and are part of the backbone of traditional therapies [10]. The diversity of molecular structures from natural origins is responsible for the pronounced biological potential presented by these molecules, which represent a promising source of new drug leads [9].

Currently, many of the available drugs for parasitic disease treatment are NPs or derivatives [10–12]. Despite the fact that most of these molecules were isolated from terrestrial plants, for the past decades, we have been witnessing the growing advance of NPs obtained from marine sources in the field of drug discovery [13]. Indeed, marine organisms synthesize sophisticated molecules, aiming their survival in an environment with limited resources and predatory pressure [14]. Among the great diversity of marine organisms, macroalgae standout as an interesting source of bioactive molecules and is largely explored in the field of drug discovery for neglected diseases [1].

Extreme marine environments such as the Southern Ocean and the cold waters surrounding the Antarctic Peninsula are geographically and biologically isolated [15]. In Antarctica, the Desmarestiales are the main constituents of the benthic algal flora. Taxonomic studies of *Desmarestia antarctica* are well established, however, the secondary metabolites produced by this macroalga and its biological potential are poorly explored [16].

Even though progress has already been achieved in the past years in the field of NPs from polar regions, the climate conditions and remoteness of these environments still pose difficulties to the improvement of this area [17]. Moreover, another common issue regarding NPs and therapeutic lead discovery is that despite the potential results obtained in the bioassays in the initial extracts or fractions, the bioactive compounds may not be isolated or they are known molecules with established biological potential [18]. As a strategy, the use of new approaches such as MS/MS-based Global Natural Products Social (GNPS) Molecular Networking (MN) has contributed to avoiding the loss of chemical information and improved bioguided fractionation and isolation of new and bioactive molecules [19].

Herein, we report for the first time the chemical profile of volatile compounds in the macroalga *D. antarctica*. Furthermore, the antiparasitic activity of this species was evaluated against *L. amazonensis*, *N. caninum*, and *P. falciparum*, and its cytotoxicity on 3T3 BALB/c fibroblasts and Vero cells was assessed.

## Results and Discussion

The chemical profile of volatile compounds in the crude extract of *D. antarctica* was accessed using GC-MS, and the identified constituents are shown in ▶ **Table 1**. Among the identified compounds,

FAs, esters, terpenes, and sterols were the most prevalent. Twenty-five compounds were identified. The major FAs were palmitic acid (27.8 %), oleic acid (15.8 %), and myristic acid (12.0 %). Phytol (2.9 %) and neophytadiene (2.2 %) were the prevalent terpenes. The sterol composition presented fucosterol (14.5 %) as the major constituent of this class of compounds, followed by stigmasterol (7.9 %), desmosterol (1.0 %), and brassicasterol (0.3 %). Our investigation of the *D. antarctica* chemical profile corroborates with previous investigations that show palmitic acid as the most predominant FA in the Antarctic brown macroalgae *Ascoseira mirabilis, Adenocystis utricularis*, and *Phaeurus antarcticus* [20]. The composition of macroalgal FAs varies in quality and quantity according to different environmental conditions such as light, temperature, and salinity [21, 22]. Cold-water macroalgae present a higher lipid content than tropical species [23].

In a previous study, the crude extract of *D. antarctica* presented antifouling activity against model strains of sympatric diatoms that could potentially foul it in nature [24]. However, no description of the secondary metabolites present in the extract was provided, highlighting the need to chemically characterize this macroalga species. In addition, the molecules identified in *D. antarctica* crude extract could be used as a fingerprint to future ecological studies and it is an important contribution to literature data.

The VLC fractionation of the crude extract led to nine different fractions. However, fractions DA-FA – DA-FC presented low yields, therefore only fractions DA-FD – DA-FI were used for antiparasitic activity evaluation.

In the antileishmanial assay against *L. amazonensis* promastigotes, only fraction DA-FE ($IC_{50}$ of 53.8 µg $mL^{-1}$) presented anti-promastigote activity (▶ **Fig. 1**). Cytotoxicity on 3T3 BALB/c fibroblasts (▶ **Fig. 1S**, Supporting Information) demonstrates that the DA-FE was fourfold more selective to the parasites than the reference drug amphotericin B (▶ **Table 2**).

▶ **Table 1** Chemical profile of volatile constituents identified in the *D. antarctica* crude extract obtained by GC-MS analysis (%) of total area.

| Compound | RI | ID | (%) |
|---|---|---|---|
| Benzene carboxylic acid/$C_7H_6O_2$ | 1180 | MS1 [a] | 0.33 |
| Loliolide/$C_{11}H_{16}O_3$ | 1667 | MS1 [b] | 1.11 |
| Myristic acid/$C_{14}H_{28}O_2$ | 1740 | MS1 [a] | 12.00 |
| Phthalic acid, butyl undecyl ester /$C_{23}H_{36}O_4$ | 1805 | MS1 [a] | 1.25 |
| Neophytadiene/$C_{20}H_{38}$ | 1811 | MS1 [b] | 2.22 |
| 2-Pentadecanone, 6,10,14-trimethyl/ $C_{18}H_{36}O$ | 1842 | MS1 [b] | 0.59 |
| Phytol acetate/$C_{22}H_{42}O_2$ | 1847 | MS1 [a] | 1.19 |
| Palmitoleic acid/$C_{16}H_{30}O_2$ | 1928 | MS1 [a] | 1.44 |
| Palmitic acid/$C_{16}H_{32}O_2$ | 1943 | MS1 [a] | 27.81 |
| Oleic acid, methyl ester/$C_{19}H_{36}O_2$ | 2094 | MS1 [b] | 0.30 |
| Phytol/$C_{20}H_{40}O$ | 2108 | MS1 [b] | 2.19 |
| Linoleic acid/$C_{18}H_{32}O_2$ | 2115 | MS1 [a] | 1.51 |
| Cervonic acid/$C_{22}H_{32}O_2$ | 2119 | MS1 [a] | 1.47 |
| Elaidic acid/$C_{18}H_{34}O_2$ | 2123 | MS1 [a] | 15.77 |
| Stearic acid /$C_{18}H_{36}O_2$ | 2141 | MS1 [a] | 0.96 |
| Arachidonic acid/$C_{20}H_{32}O_2$ | 2286 | MS1 [a] | 1.26 |
| *Cis*-5,8,11,14,17-Eicosapentaenoic acid, methyl ester/$C_{21}H_{31}O_2$ | 2299 | MS1 [a] | 1.16 |
| Elaidic acid, 2,3-dihydroxypropyl ester / $C_{21}H_{40}O_4$ | 2315 | MS1 [b] | 1.35 |
| 2-Hexadecanoyl glycerol /$C_{19}H_{38}O_4$ | 2448 | MS1 [a] | 0.42 |
| Decanedioic acid, bis(2-ethylhexyl) ester/ $C_{26}H_{50}O_4$ | 2792 | MS1 [a] | 0.17 |
| α-Tocopherol/$C_{29}H_{50}O_2$ | 3120 | MS1 [a] | 0.11 |
| Stigmasterol/$C_{29}H_{48}O$ | 3205 | MS1 [a] | 7.90 |
| Brassicasterol/$C_{28}H_{46}O$ | 3235 | MS1 [a] | 0.33 |
| Fucosterol/$C_{29}H_{48}O$ | 3299 | MS1 [b] | 14.56 |
| Desmosterol/$C_{27}H_{44}O$ | 3468 | MS1 [b] | 1.09 |

RI: relative retention index, ID: identification by GC-MS fragmentation profile, MS1 [a]: Nist11.lib, MS1 [b]: Wiley7.lib.

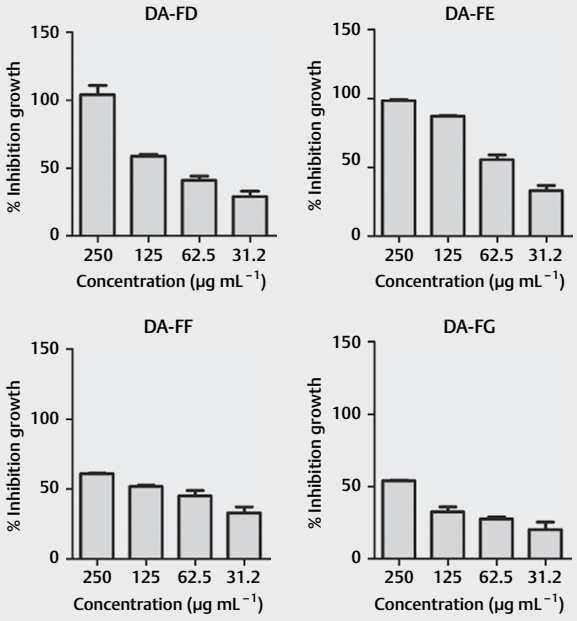


▶ **Fig. 1** Inhibition growth (%) of *L. amazonensis* promastigotes after treatment with different concentrations (µg $mL^{-1}$) of fractions DA-FD, DA-FE, DA-FF, and DA-FG. The results are expressed as the mean (n = 3) ± SD of three independent experiments.

▶ **Table 2** Anti-*L. amazonensis* promastigote activity and 3T3 BALB/c fibroblast cytotoxicity of the crude extract and fractions from *D. antarctica.*

| Sample | $IC_{50\text{-}PRO}$[a] (µg $mL^{-1}$; mean ± SD) | $IC_{50\text{-}BALB/c}$[b] (µg $mL^{-1}$; mean ± SD) | SI[c] |
|---|---|---|---|
| Crude extract | > 500 | 815.6 ± 2.7 | – |
| DA-FD | 96.5 ± 5.5 | 115.2 ± 1.1 | 1.1 |
| DA-FE | 53.8 ± 4.4 | 179.1 ± 1.4 | 3.3 |
| DA-FF | 102.2 ± 5.7 | 134.0 ± 1.1 | 1.3 |
| DA-FG | 223.2 ± 9.7 | – | – |
| DA-FH | > 250 | 138.7 ± 1.2 | 2.4 |
| DA-FI | > 250 | – | – |
| Amphotericin B | 5.8 ± 0.8 | 4.6 ± 1.0 | 0.8 |

[a]Antiparasitic activities are expressed as half-maximal inhibitory concentrations ($IC_{50\text{-}PRO}$), and [b]mammalian cell toxicities are expressed as half-maximal cytotoxic concentrations ($IC_{50\text{-}BALB/c}$). [c]The selectivity index was calculated as the $IC_{50\text{-}BALB/c}/IC_{50\text{-}PRO}$.

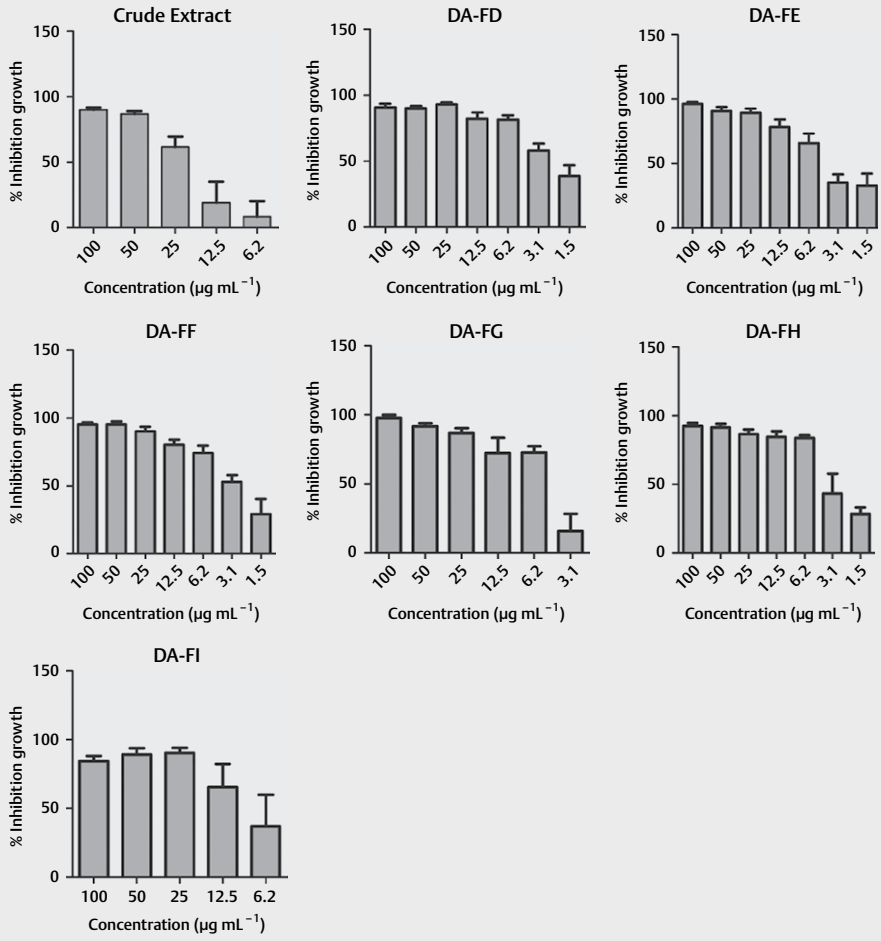


▶ **Fig. 2** Inhibition growth (%) of *N. caninum* tachyzoites after treatment with different concentrations (μg $mL^{-1}$) of the crude extract and fractions DA-FD, DA-FE, DA-FF, DA-FG, DA-FH, and DA-FI. The results are expressed as the mean (n = 3) ± SD of three independent experiments.

▶ **Table 3** Anti-*N. caninum* tachyzoites activity and Vero cell cytotoxicity of the crude extract and fractions from *D. antarctica.*

| Sample | $IC_{50\text{-}TAC}$[a] (μg $mL^{-1}$; mean ± SD) | $CC_{50\text{-}VERO}$[b] (μg $mL^{-1}$; mean ± SD) | SI[c] |
|---|---|---|---|
| Crude extract | 20.6 ± 6.3 | 75.1 ± 22.6 | 3.6 |
| DA-FD | 1.6 ± 1.3 | 44.5 ± 21.3 | 27.8 |
| DA-FE | 4.2 ± 2.4 | > 100 | 23.8 |
| DA-FF | 3.1 ± 2.1 | 71.9 ± 16.6 | 23.2 |
| DA-FG | 5.5 ± 1.3 | > 100 | 18.2 |
| DA-FH | 3.1 ± 2.0 | 40.1 ± 6.9 | 12.9 |
| DA-FI | 12.5 ± 17.2 | 87.3 ± 57.2 | 7.0 |
| Pyrimethamine | 0.7 | – | – |

[a]Antiparasitic activities are expressed as half-maximal inhibitory concentrations ($IC_{50\text{-}TAC}$), and [b]mammalian cell toxicities are expressed as half-maximal cytotoxic concentrations ($CC_{50\text{-}VERO}$). [c]The selectivity index was calculated as the $IC_{50\text{-}VERO}/IC_{50\text{-}TAC}$,

Results indicated that all fractions significantly inhibited the proliferation of *N. caninum* tachyzoites (▶ **Fig. 2**). Among these fractions, DA-FD, DA-FE, DA-FF, and DA-FH demonstrated $IC_{50}$ values below 5.5 μg $mL^{-1}$ on *N. caninum* (1.6 μg $mL^{-1}$, 4.2 μg $mL^{-1}$ 3.1 μg $mL^{-1}$, and 3.1 μg $mL^{-1}$, respectively). On the other hand, DA-FI and the crude extract presented the lowest capacities to inhibit *N. caninum* with $IC_{50}$ values of 12.5 μg $mL^{-1}$ and 20.6 μg $mL^{-1}$, respectively (▶ **Table 3**). All fractions demonstrated higher $CC_{50}$ values on Vero cells compared to $IC_{50}$ values on *N. caninum* tachyzoites. No toxic effects were observed for concentrations below 40 μg $mL^{-1}$ (▶ **Table 3** and ▶ **Fig. 2S**, Supporting Information). The $CC_{50}$ value was used to calculate the SI, which represents the relation between the cytotoxicity and the anti-parasite concentrations ($CC_{50}/IC_{50}$), indicating the effectiveness and safety of a compound for further *in vivo* applications. Among the fractions, DA-FD indicated the highest SI (27.8), followed by DA-FE (> 23.8), DA-FF (23.2), DA-FG (> 18.2), DA-FH (12.9), DA-FI (7.0), and the crude extract (6.6) (▶ **Table 3**).

Results presented fraction DA-FD as the most active in the anti-*Neospora* evaluation. Concerning this bioactivity, DA-FD was

screened against *P. falciparum* and showed promising antiplasmodial activity ($IC_{50}$ of 19.1 µg $mL^{-1}$) (▶ **Table 4** and ▶ **Fig. 3**).

The volatile constituents of the most active fractions in the antiparasitic bioassays were identified using GC-MS analysis and are shown in ▶ **Table 5**. The fractions DA-FD, DA-FE, DA-FF, and DA-FH presented promising antiparasitic effects. The major identified compounds in fraction DA-FD were palmitic acid (29.3 %), myristic acid (21.3 %), fucosterol (8.8 %), oleic acid, methyl ester (3.2 %), and desmosterol (2.8 %). Myristic acid (14.9 %) and oleic acid (12.6 %) represent the major FAs in fraction DA-FE. In fraction DA-FF, the major constituents were phthalic acid, di(2-methylbutyl) ester (27.0 %), loliolide (15.1 %), phytol acetate (4.2 %), and neophytadiene (4.0 %). Fraction DA-FH presented loliolide (16.7 %) as the major compound, followed by neophytadiene (15.3 %), tetradecanal (8.0 %), phytol acetate (6.5 %), phthalic acid, bis(2-ethylhexyl) ester (6.1 %), and 2-pentadecanone, 6,10,14-trimethyl (3.2 %).

Continuing our efforts to chemically characterize the bioactive fractions in the *N. caninum* assay, we used the data generated through LC-MS/MS analysis to construct a bioactivity-based MN of *D. antarctica*. After the data process, the ions that presented r > 0.65 and p value < 0.1 (larger nodes) were pointed as the bioactive components and are presented as larger nodes in ▶ **Fig. 4**. The GNPS library was used to identify annotated molecules. However, none of the ions were identified. In ▶ **Table 6**, we summarize the ions that were presented as bioactive and present probable molecular formulas of these molecules.

▶ **Table 4** Antiplasmodial activity in *P. falciparum* trophozoites and cytotoxicity in 3T3 BALB/c fibroblasts of the DA-FD fraction from *D. antarctica*.

| Sample | $IC_{50\text{-}TRO}$[a] (µg $mL^{-1}$; mean ± SD) | $IC_{50\text{-}BALB/c}$[b] (µg $mL^{-1}$; mean ± SD) | SI[c] |
|---|---|---|---|
| DA-FD | 19.1 ± 3.9 | 115.2 ± 1.1 | 6.0 |
| Chloroquine diphosphate | 0.1 ± 0.3 | – | – |

[a]Antiparasitic activities are expressed as half-maximal inhibitory concentrations ($IC_{50\text{-}TRO}$), and [b]mammalian cell toxicities are expressed as half-maximal cytotoxic concentrations ($IC_{50\text{-}BALB/c}$). [c]The selectivity index was calculated as the $IC_{50\text{-}BALB/c}/IC_{50\text{-}TRO}$.

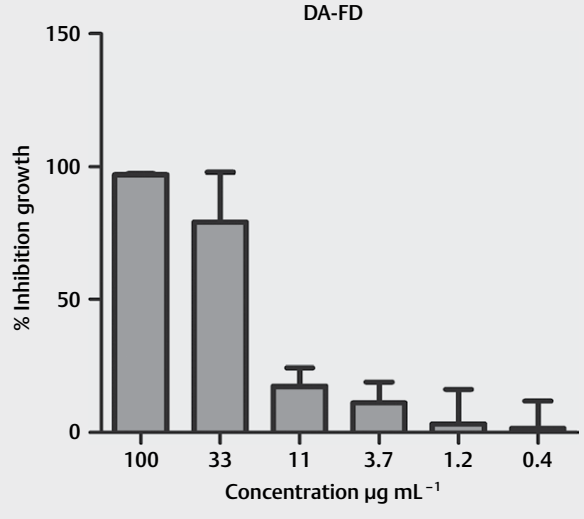


▶ **Fig. 3** Inhibition growth (%) of *P. falciparum* trophozoites after treatment with different concentrations (µg $mL^{-1}$) of fraction DA-FD. The results are expressed as the mean (n = 3) ± SD of two independent experiments.

The FAs present antibacterial properties due their ability to kill or inhibit the growth of bacteria, and are used by many organisms as defense against parasitic or pathogenic bacteria [25]. Fucosterol is the characteristic sterol of brown macroalgae [26]. Previous studies report the antileishmanial activity of fucosterol isolated from the brown macroalga *Lessonia vadosa* towards amastigotes of *Leishmania infantum* ($IC_{50}$ of 10 µM, SI > 10) and *L. amazonensis* ($IC_{50}$ of 8 µM, SI > 12), despite the lower activity when compared to amphotericin B ($IC_{50}$ of 0.2 µM). The higher SI values of fucosterol turn it into a promising lead for the development of leishmanicidal drugs with less toxic effects [27]. Fucosterol isolated from the brown macroalgae *Sargassum linearifolium* also exerted high inhibitory effects against 3D7 chloroquine sensitive *P. falciparum* ($IC_{50}$ of 7.48 µg $mL^{-1}$), and morphological changes of *P. falciparum* were observed [28].

Phthalates have been isolated from *Brevibacterium mcbrellneri* and showed bactericidal and mosquito larvicidal activities [29]. A study reporting the antileishmanial potential of the Antarctic red alga *Irideae cordata* against *L. amazonensis* amastigotes led to the identification of phthalic acid, diisobutyl ester, phthalic acid, di(2-methylbutyl) ester and palmitic acid beta-monoglyceride in the most active fractions of *I. cordata* through GC-MS analysis [17]. Loliolide is found in many macroalgae and plants and its biological activity has been described as a repellent [30] and inducer of herbivore resistance [31]. The active hexane and dichloromethane fractions of the red macroalgae *Centroceras clavulatum* against *Trypanosoma cruzi* forms (epimastigote $IC_{50}$ of 19.1 µg $mL^{-1}$ and trypomastigote $IC_{50}$ of 76.2 µg $mL^{-1}$) were analyzed through GC-MS and compounds such as loliolide, neophytadiene, and phytol were identified [32]. The antiparasitic activity of phytol against *Schistosomiasis mansoni* has been described. *In vitro,* phytol reduced the motor activity of worms, caused by their death. *In vivo*, a single dose of phytol (40 mg/kg) administered orally to mice infected with adult *S. mansoni* resulted in total and female worm burden reductions of 51.2 and 70.3 %, respectively [33]. A previous study has identified neophytadiene in cytotoxic fractions of *Senna* spp. (Leguminosae, Caesalpinioideae) tested against human colon and human glioblastoma cell lines [34]. Interestingly, the increase of neophytadiene concentration in fraction DA-FH (15.3 %) compared to DA-FF (3.9 %) led to higher cytotoxic effects in Vero cells. The fractions of *D. antarctica* demonstrated low toxicity in the tested mammal cells.

Despite the advances for the screening of drug candidates against *N. caninum*[35], there are few works reporting the bioactivity of NPs against this parasite. Only plant extracts such as Thai Piperaceae, *Thalassomya japonica*, and *Sophora flavescens* were screened to date [36, 37]. Comparatively, the *D. antarctica* extract and fractions demonstrated a lower $IC_{50}$ in relation to the Thai piperaceae extract ($IC_{50}$ 22.1 µg $mL^{-1}$).

To our knowledge, there is no reports concerning the use of macroalgae secondary metabolites against *N. caninum*. In this way, this work reveals the novelty of macroalgae use to treat *N. caninum*

▶ **Table 5** Chemical profile of volatile constituents identified in DA-FD, DA-FE, DA-FF, and DA-FH obtained by GC-MS analysis (%) of the total area.

| Compounds | RI/*ID* | Peak area (%) | | | |
|---|---|---|---|---|---|
| | | DA-FD | DA-FE | DA-FF | DA-FH |
| *Trans*-2-Heptenal/$C_7H_{12}O$ | 780/*b* | 0.15 | 0.22 | 0.57 | – |
| 1,4-Hexadiene, 3-ethyl/$C_8H_{14}$ | 999/*a* | – | – | 0.18 | – |
| *Trans*-6-Tetradecene/$C_{14}H_{28}$ | 1053/*a* | – | – | 0.28 | – |
| 6-Undecanone/$C_{11}H_{22}O$ | 1085/*b* | – | 0.35 | – | – |
| Nonanal/$C_9H_{18}O$ | 1112/*a* | 0.15 | – | 0.35 | 0.24 |
| 2-Ethyl-3-methylmaleimide/$C_7H_9NO_2$ | 1192/*b* | 0.13 | – | 0.67 | – |
| *Trans*-Decenal/$C_{10}H_{18}O$ | 1254/*a* | 0.57 | 0.25 | 1.43 | 1.52 |
| Heptanoic acid, anhydride/$C_{14}H_{26}O_3$ | 1277/*a* | – | 0.85 | 0.11 | – |
| *Trans*-2,*Cis*-4-Decadienal/$C_{10}H_{16}O$ | 1283/*b* | – | – | 0.13 | – |
| *Trans*-2-Decen-1-ol/$C_{10}H_{20}O$ | 1334/*a* | – | 0.09 | 0.42 | – |
| Dodecane, 2,6,10-trimethyl/$C_{15}H_{32}$ | 1436/*a* | 0.11 | – | 0.35 | – |
| Dihydroactinolide/$C_{11}H_{16}O_2$ | 1490/*a* | – | – | 0.36 | – |
| 2,11-Dioxatetracyclo-undec-4-ene, 3,7,7,10-tetramethyl/$C_{13}H_{18}O_2$ | 1497/*a* | – | 4.48 | – | – |
| Tetradecanal/$C_{14}H_{28}O$ | 1607/*a* | – | – | – | 8.00 |
| Loliolide/$C_{11}H_{16}O_3$ | 1667/*b* | – | 0.22 | 15.08 | 16.66 |
| Palmictoleic acid, hexadecylester/$C_{32}H_{64}O_2$ | 1715/*b* | – | – | 0.98 | – |
| Myristic acid, methylester/$C_{15}H_{30}O_2$ | 1717/*a* | 1.41 | 0.32 | – | – |
| Myristic acid/$C_{14}H_{28}O_2$ | 1740/*a* | 21.30 | 14.92 | 1.68 | – |
| Palmitic acid/$C_{16}H_{32}O_2$ | 1720/*b* | 29.31 | – | – | – |
| Neophytadiene/$C_{20}H_{38}$ | 1811/*b* | 2.31 | 1.04 | 3.97 | 15.30 |
| Elaidic acid /$C_{18}H_{34}O_2$ | 1832/*a* | – | 12.69 | – | – |
| 2–Pentadecanone, 6,10,14–trimethyl/$C_{18}H_{36}O$ | 1842/*a* | 1.79 | 2.09 | 1.31 | 3.20 |
| Phytol acetate/$C_{22}H_{42}O_2$ | 1847/*b* | – | – | 4.23 | 6.52 |
| Phthalic acid, diisobutyl ester/$C_{16}H_{22}O_4$ | 1848/*a* | – | – | 2.74 | – |
| Palmitoleic acid, methylester/$C_{17}H_{32}O_2$ | 1907/*b* | 0.44 | – | – | – |
| Palmitic acid, methylester/$C_{17}H_{34}O_2$ | 1918/*b* | 1.60 | 0.20 | – | – |
| Phthalic acid, butyl isobutyl ester/$C_{16}H_{22}O_4$ | 1978/*a* | – | – | 0.34 | – |
| 1-Nonadecene/$C_{19}H_{38}$ | 1993/*a* | 0.24 | – | – | – |
| 1,2-Oxathiane, 6-dodecyl-, 2,2-dioxide/ $C_{16}H_{32}O_3S$ | 1995/*a* | – | – | – | 0.34 |
| 1,8-Dioxacyclohexadecane-2,10-dione, 5,6:12,13-diepoxy-8,16-dimethyl/$C_{16}H_{24}O_6$ | 2037/*a* | 0.59 | – | – | – |
| Palmitic acid, 3-hydroxy-, methylester/$C_{17}H_{34}O_3$ | 2052/*a* | 0.11 | – | – | – |
| Linoleic acid, methylester/$C_{19}H_{34}O_2$ | 2088/*a* | 0.24 | – | – | – |
| Oleic acid, methylester/$C_{19}H_{36}O_2$ | 2095/*a* | 3.24 | – | – | – |
| 14$\beta$-Pregnane/$C_{21}H_{36}$ | 1906/*a* | 1.16 | 3.44 | – | – |
| Phthalic acid, di(2-methylbutyl) ester/$C_{18}H_{26}O_4$ | 1959/*b* | – | – | 27.00 | – |
| *Cis*-Phytol/$C_{20}H_{40}O$ | 2104/*b* | 0.76 | – | – | – |
| Phytol/$C_{20}H_{40}O$ | 2108/*b* | 0.66 | 1.37 | 1.56 | 2.61 |
| Palmitaldehyde, diallyl acetal/$C_{22}H_{42}O_2$ | 2137/a | 0.81 | – | – | 1.78 |
| Triacontane/$C_{30}H_{62}$ | 2323/*c* | 1.93 | 17.64 | 0.77 | – |
| Phthalic acid, bis(2-ethylhexyl) ester/$C_{24}H_{38}O_4$ | 2528/*a* | 1.17 | 2.56 | 2.42 | 6.06 |
| *Cis*-13-Docosenamide/$C_{22}H_{43}NO$ | 2627/*a* | – | – | 0.57 | – |
| $\alpha$-Tocopherol/$C_{29}H_{50}O_2$ | 3120/*a* | – | – | 0.33 | 0.76 |
| Desmosterol/$C_{27}H_{44}O$ | 3253/*a* | 2.85 | – | – | – |
| Isofucosterol/$C_{29}H_{48}O$ | 3290/*b* | 0.72 | – | – | – |
| Fucosterol/$C_{29}H_{48}O$ | 3299/*b* | 8.80 | – | – | – |

RI: relative retention index, ID: identification by GC-MS fragmentation profile, *a*Nist11.lib, *b*Wiley7.lib; *c*FFNSC1.3.lib.

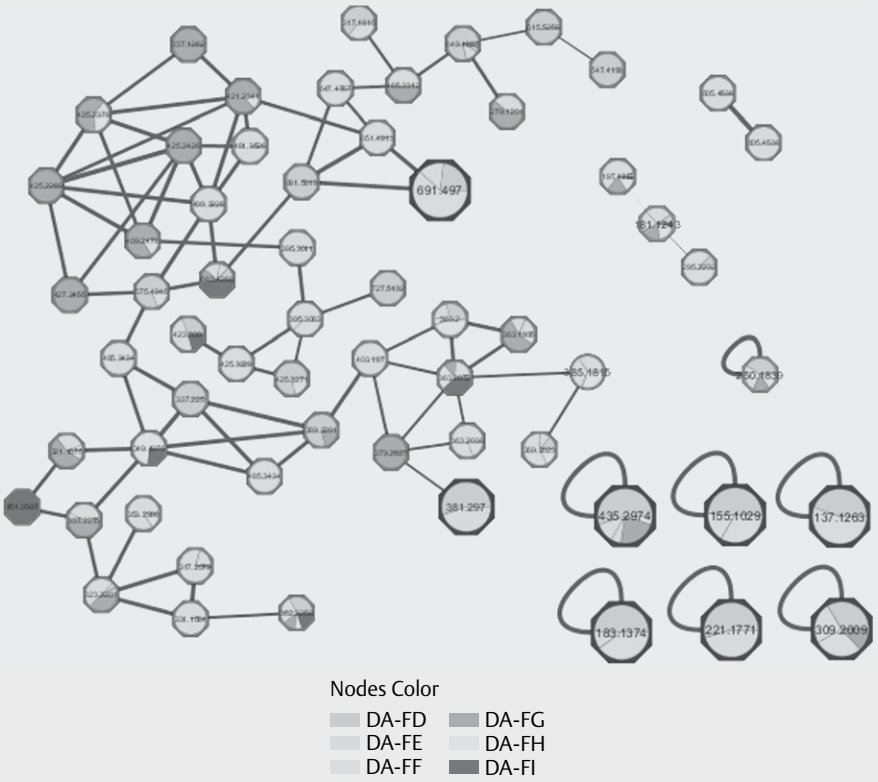


▶ **Fig. 4** Molecular networking of *D. antarctica* fractions analyzed by LC-MS in the positive ionization mode. Nodes represent detected compounds and are colored according to the type of sample. Larger node forms represent ions with a high score of bioactivities (r > 0.65 and p value < 0.1) in *N. caninum* assays. Edges between nodes represent molecular structural similarity between compounds. Nodes without GNPS spectral library matching with other nodes are represented as self-loops.

infections. Thus, the use of macroalgae derivatives may be a promising strategy to develop forms to control coccidian parasites in humans and animals. Moreover, special attention is necessary to develop the use of alternative sources of compounds to the *N. caninum* control, once there is no commercial strategy for the neosporosis treatment.

## Material and Methods

### Algal material

Samples of *D. antarctica* R. L. Moe & P.C. Silva Desmarestiaceae specimens were collected at King's George Island, Demay Point, Antarctica (62 °12' 60.0" S 58 °25' 59.9" W) in January 2016 during the Brazilian Antarctic Expedition OPERANTAR XXXIV. A total of 350 g of macroalga were collected and manually cleaned with local seawater to remove surface contaminants. A voucher specimen was authenticated by Dr. Beatriz Castelar Duque Estrada and MSc. Jônatas Martinez Canuto Souza and deposited in the herbarium Maria Eneyda P. Kauffman Fidalgo, Institute of Botany (São Paulo – Brazil) under number SP 470155.

### Extraction and fractionation

A sample (300 g) was fragmented and extracted (× 3) with dichloromethane ($CH_2Cl_2$):methanol (MeOH) 2:1 v/v (500 mL) for 30 min under stirring in a thermal blanket with a controlled temperature (30 °C). Solvents ($CH_2Cl_2$:MeOH) were selected to obtain both polar and nonpolar compounds. The combined resulting solutions were evaporated under reduced pressure at 30 °C, resulting in 2 g of crude extract (CE). The CE was fractionated by silica gel 60 (Mesh 70–230) VLC in a 500-mL glass Buchner funnel. Elution using the organic solvents, *n*-hexane (HX), ethyl acetate (EtOAc), and methanol (MeOH) with 300 mL of a stepwise polarity gradient yielded nine fractions: DA-FA (HX), DA-FB (HX:EtOAc, 9:1), DA-FC (HX:EtOAc, 8:2), DA-FD (HX:EtOAc, 6:4), DA-FE (HX:EtOAc, 4:6), DA-FF (HX:EtOAc, 2:8), DA-FG (EtOAc), DA-FH (EtOAc:MeOH, 7.5:2.5), and DA-FI (MeOH).

### Chemical profile of crude extract and bioactive fractions using a GC-MS approach

The GC-MS analysis was performed using a Gas Chromatograph Mass Spectrometer Mod GCMS-QP2010-Ultra (Shimadzu). Analyses were performed using a nonpolar RTx-5MS (30 m × 0.25 mm × 0.25 um) column and helium ($H_2$) as the carrier gas at a flow rate of 1 mL $min^{-1}$. The temperature was increased at the rate of 3 °C $min^{-1}$ from 60 to 260 °C and was held isothermally for 60 min.

▶ **Table 6** Molecular formula of ions indicated as bioactive (r > 0.65 and p value < 0.1) against *N. caninum*.

| RT | *m/z* | Molecular formula | Error (ppm) |
|---|---|---|---|
| 18.3 | 309.2009 | $C_{13}H_{28}N_2O_6$ | 5.3 |
| | | $C_{20}H_{24}N_2O$ | 13.7 |
| | | $C_{18}H_{28}O_4$ | 18.3 |
| 23.2 | 155.1049 | $C_5H_{10}N_6$ | 2.5 |
| | | $C_9H_{14}O_2$ | 14.8 |
| 25.5 | 381.2970 | $C_{18}H_{40}N_2O_6$ | 1.5 |
| | | $C_{23}H_{40}O_4$ | 9.1 |
| | | $C_{24}H_{36}N_4$ | 12.6 |
| | | $C_{25}H_{36}N_2O$ | 16.9 |
| 26.5 | 137.1263 | $C_{10}H_{16}$ | 8.1 |
| 27.6 | 183.1374 | $C_{11}H_{18}O_2$ | 6.0 |
| | | $C_7H_{14}N_6$ | 8.7 |
| 34.2 | 221.1771 | $C_{12}H_{20}N_4$ | 2.2 |
| | | $C_{11}H_{24}O_4$ | 8.3 |
| 34.4 | 435.2974 | $C_{23}H_{38}N_4O_4$ | 0.7 |
| | | $C_{22}H_{42}O_8$ | 3.7 |
| | | $C_{28}H_{38}N_2O_2$ | 8.6 |
| | | $C_{29}H_{38}O_3$ | 17.2 |
| 36.9 | 691.4970 | $C_{37}H_{70}O_{11}$ | 3.8 |
| | | $C_{44}H_{66}O_6$ | 4.7 |
| | | $C_{51}H_{62}O$ | 13.2 |
| | | $C_{48}H_{66}O_3$ | 17.3 |

RT: retention time in minutes, *m/z*: mass to charge ratio.

The injection and transfer line temperatures were 260 °C. The detection was carried out in the full scan mode ranging between 50 and 650 *m/z*. The ionization mode employed was electron impact (EI) with a collision energy of 70 eV, and the mass spectrometer ion source was maintained at 260 °C. The relative retention index (RI) values were calculated by evaluating external standard sets of *n*-alkanes (C9-C35) under the same conditions and column using the formula obtained by Vandendool and Kratz equation [38]. The confirmation of the compounds was obtained by comparing the calculated RI values with library matches (Wiley 7, Nist 11s, and FFNSC1.3 libraries).

## LC-MS/MS analysis and molecular networking approach

The crude extract and fractions from *D. antarctica* were analyzed on a Shimadzu UFLC system coupled to a quadrupole time-of-flight tanden mass spectrometer (micrOTOF QII, Bruker Daltonics) using a C18 Supelco column (5 µm, 15 cm × 3.0 mm; Ascenti Express C18). The mobile phase was composed of water (A) and MeOH (B), both with 0.1 % formic acid at a flow rate of 1.0 mL $min^{-1}$. The gradient was 0–35 min, 30–90 % B; 35–45 min, 90 % B; 45–55 min 90–100 % B; 55–60, min 100–30 % B; 60–65 min, 30 % B. The column oven was set at 35 °C and 20 µL of each sample were injected.

Chemical profiles were obtained in the positive ionization mode. The mass spectrometer parameters were as follow: capillary voltage 3.5 kV; end plate offset 500 V; nebulizer 5 bar; dry gas ($N_2$) flow 10 L · $min^{-1}$; dry temperature 220 °C; scan mode MS/MS (auto) between *m/z* 100 and 1500; precursor average 4; number of precursors 3; exclusion activation 1 spectra; exclusion release 36 s; charged ions group length 5.

LC-$MS^n$ data were converted to the .mzXML format using MSconvert software (Proteowizard Software Foundation) and processed using MzMineTM (BMC Bioinformatics). The following parameters were employed: mass detection using the centroid algorithm, scan MS level 1 (noise level, 1.0E3) and scan MS level 2 (noise level, 1.0E2); ADAP chromatogram builder (min group size in # of scans, 1.0E3; group intensity threshold, 1.0E3; min highest intensity, 3.0E3; *m/z* tolerance, 0.01 *m/z* or 20 ppm); chromatogram deconvolution using wavelets (ADAP) algorithm (S/N threshold, 10; S/N estimator, intensity window SN; min feature height, 3.0E3; coefficient/area threshold, 10; peak duration range, 0.02–2.00; RT wavelet range, 0.02–0.20) (*m/z* center calculation – median; *m/z* range for $MS^2$ scan pairing, 0.01; RT for $MS^2$ scan pairing, 0.2); isotopic peak grouper (*m/z* tolerance, 0.01 *m/z* or 20 ppm; retention time tolerance in minutes, 0.2; maximum charge, 2; representative isotope, most intense) and alignment using the join aligner [*m/z* tolerance, 0.02 *m/z* or 20 ppm; weight for *m/z*, 75; retention time tolerance, 0.2 (abs); weight for retention time, 25]. After data processing, peaks with the $MS^2$ scan were exported for GNPS analysis (.csv quantification spreadsheet and .mgf file).

The output data were uploaded to the GNPS platform and a feature-based MN was created, employing the following parameters: precursor ion mass tolerance, 2.0 Da; fragment ion mass tolerance, 0.5 Da; minutes pairs cos, 0.6; minimum matched fragment ions, 4; maximum shift between precursors, 500 Da; network topK, 10; maximum connected component size, 100; library search minutes matched peaks, 4; score threshold, 0.7; search analogues, don't search; maximum analog search mass difference, 100 Da; top results to report per query, 1; minimum peak intensity, 0; filter precursor window, filter; filter library, filter library; filter peaks in 500 Da window, filter; normalization per file, no norm; aggregation method for peak abundances per group, sum. The generated MN was visualized and analyzed with Cytoscape version 3.8 (Institute for Systems Biology).

The bioactivity score significance was predicted and mapped onto the MN according to Nothias et al. [18]. Briefly, the .csv spreadsheet generated by MzMine was used for the calculation of the bioactivity score for *N. caninum* and *L. amazonensis*, separately, using the selective index and an R-based Jupyter notebook available from GitHub at http://github.com/DorresteinLaboratory/Bioactive_Molecular_Networks. The output table was imported into the Cytoscape software and the nodes with r > 0.65 and p value < 0.1 were selected (larger nodes).

## Antileishmanial activity

Promastigote forms of *L. amazonensis* (MPRO/BR/1972/M1841-LV-79) were cultivated at 27 °C in liver infusion tryptose medium supplemented with 10 % FBS (Sigma-Aldrich), penicillin, and streptomycin (Sigma-Aldrich). Cultured promastigotes at the end of the exponential growth phase (6–7 days) were seeded at $1 \times 10^7$ parasites $mL^{-1}$ in 96-well flat-bottom plates (TPP; Sigma-Aldrich). Samples were dissolved in DMSO (Sigma-Aldrich) (the highest concentration was 1.4 %), then they were added to the parasite suspension at final concentrations from 7.8–500 µg $mL^{-1}$ to the crude extract

and from 3.9–250 µg $mL^{-1}$ to the fractions, and incubated at 27 °C for 72 h. Amphotericin B (purity > 95 %; Sigma-Aldrich) was used as a reference drug from 1.6–100 µg $mL^{-1}$. The assays were carried out in triplicate. The cell viability was assessed by the MTT method [39]. Briefly, the plates were kept at 28 °C for 72 h. Then, an aliquot of 10 µL of 6 mM MTT and 0.7 mM PMS (phenazine methosulfate) was added to each well, and the plates were incubated at 28 °C for 75 min. Subsequently, 100 µL of 10 % sodium dodecyl sulfate (**SDS**) were added and maintained at room temperature for 30 min, and, finally, the samples were read at 595 nm. All the incubations were performed in the dark. The 50 % of promastigote parasite growth inhibition is expressed as the inhibitory concentration ($IC_{50\text{-}PRO}$) in µg.

## Anti-neospora activity

A proliferation assay was performed as previously described [5] using *β*-galactosidase-expressing tachyzoites (NcLacZ). Briefly, purified LacZ *N. caninum* tachyzoites were distributed ($1 \times 10^3$/well) on Vero cell cultures in a 96-well plate and incubated for 2 h at 37 °C and 5 % $CO_2$ to allow the invasion after the invasion process. Seven serial dilutions (starting from 100 µg $mL^{-1}$) of the crude extract and fractions of *D. antarctica* were added to the cultures and incubated for 72 h at 37 °C and 5 % $CO_2$. Following the treatment step, the wells were washed with PBS and lysed with the lysis buffer [100 mM 4- (2-hydroxyethyl)-1-piperazineethanesulfonic acid, pH 8.0; 1 mM $CaCl_2$; 1 % Triton X-100, 0.5 % SDS; 5 mM dithiothreitol] for 1 h at 50 °C. The lysed cultures were incubated with chlorophenol red-*β*-D-galactopyranoside (CPRG) buffer (5 mM CPRG, 5 mM 2-mercaptoethanol in PBS) for 2 hat 37 °C and the plates were read with an ELISA reader (Synergy H1, Biotek) at 570 nm. Pyrimethamine (purity > 95 %; Sigma-Aldrich) was used as a control drug. The percentage of parasite inhibition and cell toxicity was calculated from the mean absorbance of samples in relation to the non-treated controls. Three independent assays were performed.

## Cytotoxicity on Vero cells

The MTT assay [40] was applied for toxicity evaluation on Vero cells. The cells were cultivated in Roswell Park Memorial Institute (RPMI) supplemented with 5 % FBS (RPMI-FBS) in 75 $cm^2$ flasks. For the MTT assay, the cultures were distributed in 96-well plates ($5 \times 10^3$/well in RPMI-FBS) and cultivated at 37 °C and 5 % $CO_2$. After cell confluence, the plates were incubated with serial dilutions of *D. antarctica* crude extract and fractions (starting from 100 µg $mL^{-1}$ in phenol-free RPMI) for 72 h, 37 °C, and 5 % $CO_2$. The media was removed, and the treated cultures were incubated with 100 µL of MTT (purity > 98 %; Sigma-Aldrich) solution (500 µg $mL^{-1}$) for 4 h, 37 °C, and 5 % $CO_2$, followed by formazan crystal dilution with DMSO. The plates were read at 570 nm in an ELISA reader (Synergy H1; Biotek), and the percentage of cytotoxicity (in relation to non-treated controls) was calculated from three independent assays. The positive control was composed of 5 % DMSO (purity > 98 %; Sigma-Aldrich), which led to > 95 % cytotoxicity compared to the non-treated group. For all groups treated with *D. antarctica* fractions, the DMSO concentration was < 1 %. From the percentages of tachyzoite/Vero cell inhibition, the $IC_{50}$ and $CC_{50}$ values were calculated using Compusyn software (http://www.combosyn.com/) [41].

## Antiplasmodial activity

*In vitro* cultures of chloroquine-resistant *P. falciparum* K1 strains (MRA-159, MR4, ATCC) were established using A + type blood cells and RPMI-1640 culture medium enriched with 10 % plasma. The *in vitro* inhibition of the growth of *P. falciparum* K1 from these cultures by DA-FD was evaluated as described previously [42]. Briefly, as the initial condition for the susceptibility assay, the synchronization of cultures with 5 % *D*-sorbitol provided young trophozoites (ring stage). The sample was diluted in DMSO (10 mg $mL^{-1}$) to aid stock solutions. Stock solutions underwent sequential dilution in culture medium (RPMI-1640), resulting in seven diluted samples with concentrations in the range of 0.13–100 µg $mL^{-1}$ (well concentrations) and final (well) DMSO concentrations of 1 %. The test solution was transferred to 96-well test plates containing parasitized red blood cells with initial 2 % hematocrit and 1 % parasitemia. The sample was evaluated in duplicate and the test plate was incubated for 48 h at 37 °C. After the incubation period, analysis of thin blood smears of the contents of each well using an optical microscope provided the parasitemia of each well. Chloroquine diphosphate (purity > 98 %; Sigma-Aldrich) was used as a control drug (0.003–2.5 µg $mL^{-1}$). Interpolation of the nonlinear curve using GraphPad Prism software permitted the calculation of estimates of the sample concentrations able to inhibit 50 % of parasite growth ($IC_{50}$) compared to drug-free controls. The $IC_{50}$ values represent the results from two independent experiments with a confidence interval of 95 %.

## Cytotoxicity on 3T3 BALB/c fibroblasts

Cytotoxicity was evaluated by the neutral red uptake method [43]. The 3T3 BALB/c fibroblasts (Banco de células do Rio de Janeiro – BCRJ, Brazil) were cultivated in DMEM (Gibco) supplemented with 10 % FBS, 4 mM glutamine, penicillin (100 IU $mL^{-1}$) and streptomycin (100 µg $mL^{-1}$). The cell suspension ($1 \times 10^5$ cells $mL^{-1}$) was seeded in 96-well plates and incubated for 24 h at 37 °C in an atmosphere of 5 % $CO_2$. The samples and the positive control were firstly dissolved in DMSO (the highest final concentration was 1 %). Next, they were diluted into eight concentrations in DMEM (5 % FBS), with the final concentration ranging from 6–100 µg $mL^{-1}$ for DA-FD, from 23–100 µg $mL^{-1}$ for DA-FH, and from 0.33–5 µg $mL^{-1}$ for amphotericin B. The positive control used was sodium lauryl sulfate (Invitrogen). After incubation, the cells were treated with the diluted samples for 24 h at 37 °C in an atmosphere of 5 % $CO_2$, then the plates were washed with PBS (pH = 7.2). The cell viability was evaluated using the neutral red uptake method, and the plates were read at 540 nm. The assays were carried in triplicate. The concentration producing 50 % of cytotoxicity is expressed as the $IC_{50}$-BALB/c value in µg $mL^{-1}$. The $IC_{50}$ and $CC_{50}$ values were calculated by nonlinear regression analysis using the software GraphPad Prism version 5.0, and are presented as the mean (n = 3) ± standard deviation (SD).

## Supporting information

Dose-response curves that support the calculation of $CC_{50}$ values of *D. antarctica* fractions on 3T3 BALB/c and *D. antarctica* crude extract and fractions on Vero cells are available as Supporting Information.

## Funding

This study had financial and logistic support from the Brazilian Antarctic Program (PROANTAR/MCT/CNPq N°64/2013), Brazilian Marine Force, National Institute of Science and Technology (INCT: BioNat), Grant # 465637/2014–0, and the State of São Paulo Research Foundation (FAPESP), Grant # 2014/50926–0 and Grant # 2017/03552–5. The authors are thankful to the University of São Paulo for providing access to necessary resources, the financial and fellowship support from the Brazilian research funding agencies Coordination of Improvement of Higher-Level Personnel (CAPES), and the National Council for Scientific and Technological Development (CNPq) for the scholarship provided, Grant #1408011/2018–4. The department of Biomolecular Sciences and the Núcleo de Pesquisas em Produtos Naturais e Sintéticos – NPPNS are acknowledged.

## Conflict of Interest

The authors declare that they have no conflict of interest.

## References

[1] Falkenberg M, Nakano E, Zambotti-Villela L, Zatelli GA, Philippus AC, Imamura KB, Velasquez AMA, Freitas RP, de Freitas Tallarico L, Colepicolo P, Graminha MAS. Bioactive compounds against neglected diseases isolated from macroalgae: A review. J Appl Phycol 2019; 31: 797–823

[2] Torres-Guerrero E, Quintanilla-Cedillo MR, Ruiz-Esmenjaud J, Arenas R. Leishmaniasis: A review. F1000Res 2017; 6: 750

[3] Antinori S, Galimberti L, Milazzo L, Corbellino M. Biology of human malaria plasmodia including Plasmodium knowlesi. Mediterr J Hematol Infect Dis 2012; 4: e2012013

[4] Kwon HJ, Kim JH, Kim M, Lee JK, Hwang WS, Kim DY. Anti-parasitic activity of depudecin on Neospora caninum via the inhibition of histone deacetylase. Vet Parasitol 2003; 112: 269–276

[5] Pereira LM, Vigato-Ferreira IC, De Luca G, Bronzon Da Costa CM, Yatsuda AP. Evaluation of methylene blue, pyrimethamine and its combination on an in vitro Neospora caninum model. Parasitology 2017; 144: 827–833

[6] World Health Organization World malaria report. 2018; Available at: https://www.who.int/malaria/publications/world-malaria-report-2018/en/ Accessed April 29, 2020

[7] Capela R, Moreira R, Lopes F. An Overview of Drug Resistance in Protozoal Diseases. Int J Mol Sci 2019; 20: 5748

[8] Phyo AP, Jittamala P, Nosten FH, Pukrittayakamee S, Imwong M, White NJ, Duparc S, Macintyre F, Baker M, Möhrle JJ. Antimalarial activity of artefenomel (OZ439), a novel synthetic antimalarial endoperoxide, in patients with Plasmodium falciparum and Plasmodium vivax malaria: An open-label phase 2 trial. Lancet Infect Dis 2016; 16: 61–69

[9] Cragg GM, Newman DJ. Natural products: A continuing source of novel drug leads. Biochim Biophys Acta 2013; 1830: 3670–3695

[10] Mbekeani AJ, Jones RS, BassasLlorens M, Elliot J, Regnault C, Barrett MP, Steele J, Kebede B, Wrigley SK, Evans L, Denny PW. Mining for natural product antileishmanials in a fungal extract library. Int J Parasitol Drugs Drug Resist 2019; 11: 118–128

[11] Dutcher JD, Dutcher D. The discovery and development of amphotericin B. Dis Chest 2007; 54: 296–298

[12] Su X, Miller LH. The discovery of artemisinin and Nobel Prize in Physiology or Medicine. Sci China Life Sci 2017; 176: 139–148

[13] Oliveira de ALL, Felício de R, Debonsi HM. Marine natural products: Chemical and biological potential of seaweeds and their endophytic fungi. Rev Bras Farmacogn 2012; 22: 906–920

[14] McClintock JB, Baker BJ. Marine Chemical Ecology. 1st edition. Boca Raton: CRC Press; 2001

[15] McClintock JB, Amsler CD, Baker BJ. Overview of the chemical ecology of benthic marine invertebrates along the western Antarctic peninsula. Integr Comp Biol 2010; 50: 967–980

[16] Moe RL, Silva PC. Desmarestia antarctica (Desmarestiales, Phaeophyceae), a new ligulate Antarctic species with an endophytic gametophyte. Plant Syst Evol 1989; 164: 273–283

[17] Rangel KC, Debonsi HM, Clementino LC, Graminha MAS, Vilela LZ, Colepicolo P, Gaspar LR. Antileishmanial activity of the Antarctic red algae Iridaea cordata (Gigartinaceae; Rhodophyta). J Appl Phycol 2019; 31: 825–834

[18] Nothias LF, Nothias-Esposito M, Da Silva R, Wang M, Protsyuk I, Zhang Z, Sarvepalli A, Leyssen P, Touboul D, Costa J, Paolini J, Alexandrov T, Litaudon M, Dorrestein PC. Bioactivity-based molecular networking for the discovery of drug leads in natural product bioassay-guided fractionation. J Nat Prod 2018; 81: 758–767

[19] Philippus AC, Zatelli GA, Wanke T, Gabriela De Barros MA, Kami SA, Lhullier C, Armstrong L, Sandjo LP, Falkenberg M. Molecular networking prospection and characterization of terpenoids and C15-acetogenins in Brazilian seaweed extracts. RSC Adv 2018; 8: 29654–29661

[20] Teixeira TR, Santos GS, Turatti ICC, Paziani MH, von Zeska Kress MR, Colepicolo P, Debonsi HM. Characterization of the lipid profile of Antarctic brown seaweeds and their endophytic fungi by gas chromatography–mass spectrometry (GC–MS). Polar Biol 2019; 42: 1431–1444

[21] Filimonova V, Gonçalves F, Marques JC, De Troch M, Gonçalves AMM. Fatty acid profiling as bioindicator of chemical stress in marine organisms: A review. Ecol Indic 2016; 67: 657–672

[22] Dethier MN, Sosik E, Galloway AWE, Duggins DO, Simenstad CA. Addressing assumptions: Variation in stable isotopes and fatty acids of marine macrophytes can confound conclusions of food web studies. Mar Ecol Prog Ser 2013; 478: 1–14

[23] Miyashita K, Mikami N, Hosokawa M. Chemical and nutritional characteristics of brown seaweed lipids: A review. J Funct Foods 2013; 5: 1507–1517

[24] Amsler CD, Okogbue IN, Landry DM, Amsler MO, McClintock JB, Baker BJ. Potential chemical defenses against diatom fouling in Antarctic macroalgae. Bot Mar 2005; 48: 318–322

[25] Desbois AP, Smith VJ. Antibacterial free fatty acids: Activities, mechanisms of action and biotechnological potential. Appl Microbiol Biotechnol 2010; 85: 1629–1642

[26] Bouzidi N, Daghbouche Y, El Hattab M, Aliche Z, Culioli G, Piovetti L, Garrigues S, de la Guardia M. Determination of total sterols in brown algae by Fourier transform infrared spectroscopy. Anal Chim Acta 2008; 616: 185–189

[27] Becerra M, Boutefnouchet S, Córdoba O, Vitorino GP, Brehu L, Lamour I, Laimay F, Efstathiou A, Smirlis D, Michel S, Kritsanida M, Flores ML, Grougnet R. Antileishmanial activity of fucosterol recovered from Lessonia vadosa Searles (Lessoniaceae) by SFE, PSE and CPC. Phytochem Lett 2015; 11: 418–423

[28] Perumal P, Sowmiya R, Prasanna Kumar S, Ravikumar S, Deepak P, Balasubramani G. Isolation, structural elucidation and antiplasmodial activity of fucosterol compound from brown seaweed, Sargassum linearifolium against malarial parasite Plasmodium falciparum. Nat Prod Res 2018; 32: 1316–1319

[29] Rajamanikyam M, Vadlapudi V, Parvathaneni SP, Koude D, Sripadi P, Misra S, Amanchy R, Upadhyayula SM. Isolation and characterization of phthalates from Brevibacterium mcbrellneri that cause cytotoxicity and cell cycle arrest. EXCLI J 2017; 16: 375–387

[30] Okunade AL, Wiemer DF. -)-Loliolide, an ant-repellent compound from Xanthoxyllum setulosum. J Nat Prod 1985; 48: 472–473

[31] Murata M, Nakai Y, Kawazu K, Ishizaka M, Kajiwara H, Ab H, Takeuchi K, Ichinose Y, Mitsuhara I, Mochizuki A. Seoa S. Loliolide, a carotenoid metabolite, is a potential endogenous inducer of herbivore resistance. Plant Physiol 2019; 179: 1822–1833

[32] Rocha OP, De Felício R, Rodrigues AHB, Ambrósio DL, Cicarelli RMB, De Albuquerque S, Young MCM, Yokoya NS, Debonsi HM. Chemical profile and biological potential of non-polar fractions from Centroceras clavulatum (C. Agardh) Montagne (Ceramiales, Rhodophyta). Molecules 2011; 16: 7105–7114

[33] de Moraes J, de Oliveira RN, Costa JP, Junior ALG, de Sousa DP, Freitas RM, Allegretti SM, Pinto PLS. Phytol, a diterpene alcohol from chlorophyll, as a drug against neglected tropical Disease Schistosomiasis mansoni. PLoS Negl Trop Dis 2014; 8: e2617

[34] Silva JGA, Silva AA, Coutinho ID, Pessoa CO, Cavalheiro AJ, Silva MGV. Chemical profile and cytotoxic activity of leaf extracts from Senna spp. from northeast of Brazil. J Braz Chem Soc 2016; 27: 1872–1880

[35] Sánchez-Sánchez R, Vázquez P, Ferre I, Ortega-Mora LM. Treatment of Toxoplasmosis and Neosporosis in Farm Ruminants: State of Knowledge and Future Trends. Curr Top Med Chem 2018; 18: 1304–1323

[36] Leesombun A, Boonmasawai S, Nishikawa Y. Effects of Thai piperaceae plant extracts on Neospora caninum infection. Parasitol Int 2017; 66: 219–226

[37] Seo HS, Kim KH, Kim DY, Park BK, Shin NS, Kim JH, Youn H. GC/MS analysis of high-performance liquid chromatography fractions from Sophora flavescens and Torilis japonica extracts and their in vitro anti-neosporal effects on Neospora caninum. J Vet Sci 2013; 14: 241–248

[38] Vandendool H, Kratz PD. A generalization of the retention index system including linear temperature programmed gas-liquid partition chromatography. J Chromatogr A 1963; 11: 463–471

[39] Dutra LA, De Almeida L, Passalacqua TG, Reis JS, Torres FAE, Martinez I, Peccinini RG, Chin CM, Chegaev K, Guglielmo S, Fruttero R, Graminha MAS, Dos Santos JL. Leishmanicidal activities of novel synthetic furoxan and benzofuroxan derivatives. Antimicrob Agents Chemother 2014; 58: 4837–4847

[40] Mosmann T. Rapid colorimetric assay for cellular growth and survival: application to proliferation and cytotoxicity assays. J Immunol Methods 1983; 65: 55–63

[41] Chou TC, Talalay P. Quantitative analysis of dose-effect relationships: the combined effects of multiple drugs or enzyme inhibitors. Adv Enzyme Regul 1984; 22: 27–55

[42] de Andrade-Neto VF, Pohlit AM, Pinto ACS, Silva ECC, Nogueira KL, Melo MRS, Henrique MC, Amorim RCN, Silva LFR, Costa MRF, Nunomura RCS, Nunomura SM, Alecrim WD, MDGC Alecrim, FCM Chaves, PPR Vieira. In vitro inhibition of Plasmodium falciparum by substances isolated from Amazonian antimalarial plants. Mem Inst Oswaldo Cruz 2007; 102: 359–365

[43] NIH National Institutes of Health. Standard operating procedure (SOP) for the BALB/c 3T3 neutral red uptake cytotoxicity test – a test for basal cytotoxicity. Appendix C. 2001 Available at: doi:https://ntp.niehs.nih.gov/iccvam/docs/acutetox_docs/guidance0801/appc2.pdf. Accessed April 29, 2020